Journal of proteome research

pubs.acs.org/jpr

Article

High Throughput UHPLC-MS-Based Lipidomics Using Vacuum Jacketed Columns

Robert S. Plumb,* Giorgis Isaac, Paul D. Rainville, Jason Hill, Lee A. Gethings, Kelly A. Johnson, Joshua Lauterbach, and Ian D. Wilson

Cite This: *J. Proteome Res.* 2022, 21, 691−701

Read Online

ACCESS | Metrics & More | Article Recommendations | Supporting Information

ABSTRACT: Reversed-phase UHPLC-MS is extensively employed for both the profiling of biological fluids and tissues to characterize lipid dysregulation in disease and toxicological studies. With conventional LC-MS systems the chromatographic performance and throughput are limited due to dispersion from the fluidic connections as well as radial and longitudinal thermal gradients in the LC column. In this study vacuum jacketed columns (VJC), positioned at the source of the mass spectrometer, were applied to the lipidomic analysis of plasma extracts. Compared to conventional UHPLC, the VJC-based methods offered greater resolution, faster analysis, and improved peak intensity. For a 5 min VJC analysis, the peak capacity increased by 66%, peak tailing reduced by up to 34%, and the number of lipids detected increased by 30% compared to conventional UHPLC. The narrower peaks, and thus increased resolution, compared to the conventional system resulted in a 2-fold increase in peak intensity as well a significant improvement in MS and MS/MS spectral quality resulting in a 22% increase in the number of lipids identified. When applied to mouse plasma samples, reproducibility of the lipid intensities in the pooled QC ranged from 1.8−12%, with no related drift in t_R observed.

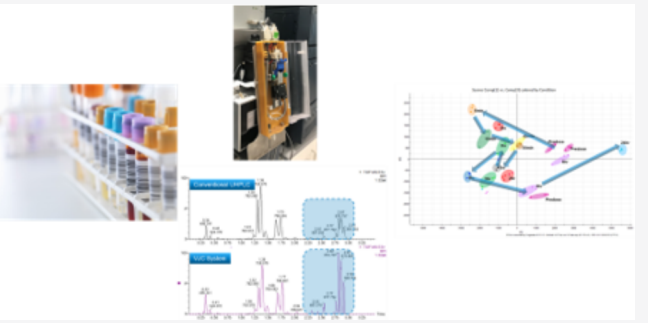

KEYWORDS: *high-throughput, lipidomics, NIST 1950 plasma, mouse plasma, gefitinib*

INTRODUCTION

As is well accepted, lipids form a class of biological molecules with many important roles and functions such as energy storage, cellular signaling, and the pathophysiology of a broad spectrum of diseases including cancer, neurodegenerative diseases, infections, diabetes, etc.[1,2] Lipidomics, which involves the comprehensive analysis of lipids of all types, can be used to detect and identify thousands of lipids across the eight common lipid classes. These classes comprise of the fatty acids, glycerolipids, glycerophospholipids, sphingolipids, saccharolipids, polyketides, sterol lipids, and prenol lipids. Using lipidomic approaches, changes in the overall phenotypes of these classes of metabolites have been seen to be consequences of many conditions. As a result, various lipids have been identified as potential biomarkers of disease. For example, Meikle et al. showed that lipidomics could be employed for risk prediction in diabetic cardiovascular disease[3] and Eghlimi et al. employed LC-MS/MS-based analysis to create two targeted lipid panels for triple negative breast cancer (TNBC).[4] Thus, a 19-lipid biomarker panel was found to be capable of distinguishing TNBC (and ES-TNBC) from controls while a 5-lipid biomarker panel enabled the differentiation of TNBC from non-TNBC. The development of such lipid-based panels usually relies upon extensive sample preparation and lengthy chromatographic analysis combined with high-resolution mass spectrometry (HRMS).[5] While this mode of analysis is ideal for discovery science, the long analysis times employed generally make it less suitable for high-throughput, large cohort, analysis. The increased interest in employing lipidomic analysis in large scale drug discovery, clinical, and epidemiological studies means that there is a need for robust high-throughput, sensitive, and highly reproducible methodologies which can be used for longitudinal studies and can be readily transferred between laboratories.[6]

Comprehensive lipid analysis by LC-MS relies upon the resolving power of the chromatography system and the specificity of the mass spectrometer to separate, detect, and identify as many of the lipid species in the sample as possible. Liquid chromatography is the preferred platform for lipid analysis, due to its resolving power, compatibility with electrospray ionization (ESI) for mass spectrometry, and the

Special Issue: Metabolomics Research

Received: October 21, 2021
Published: December 30, 2021

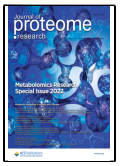

fact that the samples do not require derivatization prior to analysis.[7] The two main modes of UHPLC-MS used for lipid analysis are hydrophilic interaction liquid chromatography (HILIC) and reversed-phase (RP) LC. In HILIC methods the lipids elute as classes with elution based on the polar headgroup of the specific analytes. In practice this means that the more aliphatic lipids, such as triglycerides and cholesterol esters, elute early with the more polar lipids such as the phosphorylated species (i.e., PA, PI, and LPA) eluting later in the separation.[8] In the RP-mode retention is dependent upon the hydrophobicity of the lipid's aliphatic chains. The advantage of RP analysis is that it provides a higher resolution separation than HILIC, with narrower peaks and a greater mass loading capacity. The introduction of sub-2-μm particle chromatography (UHPLC) in the early 2000s allowed for faster, higher resolution chromatography than conventional HPLC. As a consequence of the advantages provided by UHPLC, in terms of sensitivity and increased feature detection, it rapidly displaced conventional HPLC and is currently the platform of choice for omics analysis (proteomics, lipidomics, metabol/n/omics).[9] However, it has proved to be difficult to realize the maximum performance of UHPLC when combined with MS due to the dispersion resulting from the on-column and extra-column band broadening present in the system. The extra-column band broadening largely results from the tubing connecting the LC and MS and the connections within the MS probe causing wider peaks and reduced resolution. This has been addressed, to some extent, in "chip" capillary LC analysis where the column is placed at, or in, the source of the mass spectrometer.[10] However, another significant source of band broadening is due to the frictional heating caused by the mobile phase as it passes through the column bed. This frictional heating produces radial and longitudinal temperature gradients, with the former causing velocity heterogeneity, and band broadening, with peak distortion and tailing as a result. Gritte et al., in a series of publications,[11−13] have demonstrated that the use of vacuum jacketed column (VJC) apparatus, and replacement of the column end-nuts with face sealing columns, can mitigate these deleterious effects. We recently applied this VJC approach to the rapid profiling of acetaminophen (paracetamol) and its metabolites, as well as endogenous metabolites, excreted in human urine.[14] This investigation revealed that the use of the VJC columns resulted in a 2-fold increase in peak capacity, faster analysis and up to a 100% increase in peak response compared to conventional UHPLC on the same system. Here we demonstrate the application of VJC-based UHPLC-MS to the analysis of lipids in the NIST 1950 human plasma, a bovine liver extract and also samples of mouse plasma obtained following the administration of gefitinib, an EGFR inhibitor used for certain breast, lung, and other cancers.

MATERIALS AND METHODS

Materials

LC-MS grade water, isopropanol (IPA), methanol (MeOH), acetonitrile (ACN), ammonium acetate, formic acid (FA), and leucine enkephalin (LeuEnk) were sourced from Thermo Fisher Scientific (Franklin, USA). Sodium formate, used to calibrate the time-of-flight (TOF) mass spectrometer, was sourced from Waters Corp. (Milford, USA). Distilled water was prepared in-house using Millipore System (Millipore, Burlington, MA). Metabolites in human plasma NIST SRM 1950 (NIST 1950) was obtained from Millipore Sigma (Darmstadt, Germany). The differential ion mobility system suitability Lipidomix, SPLASH Mix, and bovine liver extract were sourced from Avanti Polar Lipids (Birmingham, AL, USA).

Mouse Plasma Samples

Plasma samples were obtained as part of a study (described in detail elsewhere[15]) of the metabolism and pharmacokinetics of gefitinib in 9-week-old male C57Bl/6JRj mice (20.3−26.5 g) performed by Evotec SAS (Toulouse, France). Briefly, mice were administered the drug via both IV (10 mg/kg) and PO (50 mg/kg) routes. Each animal was sampled from the tail vein twice during the course of the study with 50 μL (100 μL at termination) of blood taken at predose, and for both IV and PO administration, at 0.10, 0.25, 0.5, 0.75, 1, 2, 3, 8, and 24 h postdose (2 mice/time point). Plasma samples were stored at −80 °C until analyzed. The study was performed after full management review, and according to both National and EU guidelines.

System Suitability

The differential ion mobility system suitability Lipidomix was used as a system suitability test (SST) to evaluate instrument performance. The mixture contains 1 mg/mL of each of a range of lipids and 0.25 mg/mL of phosphoinositide (PI 14:1). For use as a SST a solution containing 1000 ng/mL of these lipids (250 ng/mL PI) was prepared in IPA:ACN (1:1 v/v). The SST, which was analyzed prior to the commencement of analysis was used to determine mass accuracy, retention time reproducibility and LC peak intensity. The acceptance criteria were set at ±5 ppm mass accuracy, 0.1 min retention time variation and ±10% peak intensity.

Plasma Sample Preparation

NIST 1950 and mouse plasma samples (20 μL) were mixed with 100 μL of precooled (4 °C) IPA to precipitate the plasma proteins. For mouse samples, in cases where the volume available was less than 20 μL, the sample:solvent ratio was maintained at (1:5 v/v). Samples were then vortex mixed (60 s) and placed in a freezer (−20 °C, 10 min) after which they were again vortex mixed (60 s) before being left at 4 °C (120 min) to ensure complete protein precipitation. After centrifugation (10 300g, 10 min, 4 °C) the supernatant was diluted 1:5 with IPA:ACN (1:1 v/v) and transferred to Total Recovery UPLC Vials (Waters Corp., Milford, USA) and randomized prior to UHPLC-MS analysis. Each sample was analyzed in triplicate. A batch QC, used to monitor the performance of the analysis,[16] was constructed by pooling 10 μL of plasma from each time point. The resulting QC mixture was then processed as described above, with a QC analysis being performed prior to the beginning of the analysis and then following every 15th sample.

Chromatography

Samples were analyzed using a Waters ACQUITY UPLC I-Class PLUS system fitted with a flow through needle (Waters Corp., Milford, USA). A 2 μL injection of each sample was employed for all analyses. Separations were performed either on "conventional" 2.1 × 30 mm, 2.1 × 50 mm, 2.1 × 100 mm ACQUITY CSH 1.8 μm C_{18} columns or using vacuum jacketed stainless-steel 2.1 × 30 mm, 2.1 × 50 mm, 2.1 × 100 mm ACQUITY CSH C_{18} 1.8 μm C_{18} columns (Waters Corp., Milford, USA). All columns were packed using the same batch

https://doi.org/10.1021/acs.jproteome.1c00836
J. Proteome Res. 2022, 21, 691−701

Table 1. Chromatographic Conditions for 10 min/100 mm, 5 min/50 mm, and 3 min/30 mm Column Analysis

time (min) 10 min/100 mm	time (min) 5 min/50 mm	time (min) 3 min/30 mm	flow (mL/min)	%A	%B
initial	initial	initial	0.5	50	50
0.5	0.25	0.16	0.5	47	53
4	2	1.3	0.5	45	55
7	3.5	2.3	0.5	35	65
7.5	3.75	2.5	0.5	20	80
10	5	3.3	0.5	1	99
11	6	4	0.5	1	99

of stationary phase and the columns were packed on the same day (in the same column packing operation). Both the conventional and VJC columns employed the same stainless steel tubing but the VJC columns were fitted with a vacuum jacket. In addition, for the VJC columns the end nuts were replaced with face seal fittings, as described by Grittee et al.[12]

The conventional columns were housed in a Waters ACQUITY UPLC column manager thermostatically controlled to 55 °C and connected to the mass spectrometer using standard fittings (50 cm of 100 μm ID tubing from the column to the probe, and 35 cm of 120 μm tubing within the probe). Vacuum jacketed columns were housed in a prototype column holder located on the source of the mass spectrometer. In this configuration the column effluent was transferred to the MS probe via a single length of capillary tubing (6 cm of 50 μm ID tubing from the column to the probe followed by a 35 cm length of 75 μm ID within the probe). The VJC inlet temperature was 70 °C with an outlet temperature of 80 °C.

The mobile phases used for chromatography comprised ACN:H_2O:1 M aqueous ammonium formate (600:390:10 v/v) containing 0.1% FA (mobile phase A) and IPA/ACN/1 M aqueous ammonium formate (900:90:10 v/v) containing 0.1% FA (mobile phase B). The solvent was delivered at flow rate of 0.5 mL/min for either 3, 5, or 10 min for the 30, 50, and 100 mm columns, respectively, with columns eluted using the multilinear gradients detailed in Table 1.

MS data were collected for 4, 6, and 11 min for the 30, 50, and 100 mm column separations, respectively. This methodology was adapted from that previously described.[17,18]

Mass Spectrometry

MS data were acquired on a Xevo G2-XS QToF (Waters Corporation, Wilmslow, UK) using positive and negative ion electrospray ionization (+ve ESI, −ve ESI) at capillary voltages of 3.0 kV for +ve ESI and 2.5 kV for −ve ESI. The source temperature was 100 °C and the cone gas (N_2) flow was 50 L/h. The desolvation gas (N_2) flow was 600 L/h at a temperature of 300 °C, with desolvation and nebulizer gas set at 6 bar. MS experiments were performed over the m/z range 50−1200 Da. Sodium formate was used for the calibration of the TOF region. These data were collected in continuum mode using a low collision energy of 4 eV (function 1) with a collision energy ramp (19 to 45 eV) used to obtain elevated energy data (function 2). Both functions used a scan time of 0.1 s, providing the best compromise between the number of points acquired across chromatographic peaks together with the ion statistics required for mass accuracy. LeuEnk (m/z 556.2771) was used as the external lock mass with a scan collected every 30 s at a cone voltage of 40 V.

Data Analysis

The data were collected using MassLynx vs 4.1 (Waters Corp., Wilmslow, UK), while data processing and visualization was conducted using Progenisis QI vs 3.0 (Nonlinear Dynamics, Newcastle-upon-Tyne, UK). The multivariate statistical analyses were performed on EZInfo vs 2.0 (Sartorius, Gottingen, Germany). Principle components analysis (PCA) was performed using Pareto scaling over the data range of 0−3 min for the 3 min, 0−6 min for the 5 min, and 0−11 min for the 10 min UHPLC-MS analyses, respectively. Orthogonal Projections to Latent Structures Discriminant Analysis (OPLS-DA) was also performed on performed on selected data as indicated in the text for the PO samples Predose and 3 h using EZInfo vs 2.0 software. Putative lipid identification was performed using a combination of online databases searches (Lipidblast, UC Davis, San Diego, CA), and Lipid Maps (Lipidomics Gateway, https://www.lipidmaps.org) using a precursor tolerance of 10 ppm and product ion tolerance of 15 ppm and examination of the database suggestions against the mass spectral data (accurate mass of their precursor ions, fragment ion match and isotopic pattern) of individual compounds. The MS lipidomics data described in this manuscript have been uploaded to the Metabolights data repository (EMBL-EBI, Wellcome Genome Campus, Cambridgeshire, UK) with the data set identifier MTBLS3809.

RESULTS AND DISCUSSION

Chromatography

As discussed in the Introduction, the narrow peaks produced by rapid gradient UHPLC methodologies are susceptible to peak tailing and broadening resulting from the dispersion caused by postcolumn tubing and on-column thermal effects.[12,13] These effects limit the overall resolving power of the LC system. Vacuum jacketed columns, located at the source of the mass spectrometer (to minimize connecting tubing volumes), were developed to reduce these deleterious effects.[12] Additionally, it is possible to compensate for temperature changes between the inlet and outlet of the column, due to the frictional heating of the mobile phase, and remove this source of band broadening, by directly heating the two ends of the column. Postcolumn effects are then minimized by transferring the column effluent via a single short length of capillary tubing to the mass spectrometer sprayer thereby reducing post column dispersion. Recently we applied this approach to the rapid, 75 and 37 s analyses, with steep solvent gradients, of drug, drug metabolites, and endogenous metabolites in human urine.[14] This type of analysis resulted in peak widths as low as 0.4 s at the base and up to a 2-fold increase in peak capacity.

VJC-UHPLC vs Conventional UHPLC: 100 mm Columns and 10 min Analyses

On the basis of theoretical considerations, major gains in performance using the VJC on a separation on a 100 mm column using a 10 min separation should be realized. This is

https://doi.org/10.1021/acs.jproteome.1c00836
J. Proteome Res. 2022, 21, 691−701

because "peak crowding" is less problematic with VJC, as band broadening effects are reduced compared to a similar conventional analysis. Here, in order to determine if there were benefits in applying VJC technology to lipid analysis at conventional analytical scales and throughput, we have adapted a previously published method.[18] For this evaluation the initial experiments on the VJC system therefore involved a direct comparison of its performance with that of an identical conventional column used a 10 min method.

The first part of this comparison was undertaken using the separation of the widely used "SPLASH-Mix" lipid standard. In the +ve ESI chromatogram there were some qualitative differences in the retention times and peak shapes noted between the two separations (see Figure S1). The retention time differences were more pronounced in the "central" portion of the gradient, where the separation was almost isocratic, than at the end of the separation, where the gradient was steeper. It seems likely that the observed differences in t_R resulted from a combination of the shallow gradient and different column heating approaches for the VJC and conventional systems. In addition to differences in t_R, differences were also observed in peak width, e.g., for the PC lipid (m/z 753.6), eluting at a retention time of ca. 4.6 min, which was reduced from the 12 s obtained with conventional UHPLC to 9 s using VJC (a 30% improvement). In addition, the later eluting triglycerides (m/z 834.7 and 369.3), and lipids at 9.4 and 9.7 min (Figure S1), also showed a reduction in peak width of between 40 to 55% when using the VJC, compared to the conventional configuration. In the case of peak tailing, we observed that this was reduced for, e.g., the PC m/z 753.6 from 1.37 with the UHPLC system to 1.05 for the VJC system. Similarly, use of VJC reduced the tailing factor of the TG m/z 876.8 from 1.33 with the UHPLC system to 1.08 with the VJC system. This represents 21.2 and 18.8% reductions in tailing factors, respectively, as a result of employing the VJC. An indication of the improvement in resolution that was provided by mitigating peak tailing and both on column and extra-column band broadening, is that these results indicate that the average peak capacity increased from 65 for the conventional UHPLC separation and 103 for the VJC analysis. These results were sufficiently promising to encourage us to examine the results for more complex plasma samples.

When the separation was applied to the NIST 1950 plasma extract, again in +ve ESI mode, the VJC provided a significant qualitative improvement in the LC-MS chromatogram produced when compared to the standard approach. As can be seen from a simple visual inspection of the resulting LC-MS chromatograms (Figure S2), the VJC system produced narrower peaks, resulting in greater LC resolution, than provided by the conventional system. Specifically, the triplet of peaks eluting between 3.8 and 4.6 min were resolved into four separate peaks, with a low abundance lipid (m/z 806.58) clearly resolved in the VJC system but not visible using the conventional system. The triplet of triglyceride (TG) lipids (m/z 874.8, 876.8, and 369.3) eluting between 9.0 and 10.0 min were also fully baseline resolved by the VJC system, with a further TG lipid (m/z 829.8) being resolved from the m/z 874.8 peak at 9.4 min. There was also further fine detail revealed in the VJC/MS analysis between 5.2 and 8.3 min which was not visible in the standard UHPLC-MS separation (Figure S3). Similar results were also obtained for the separation of the triglycerides eluting between 9.25 and 9.9 min (Figure S4). An improvement in performance was also observed for the −ve negative ion ESI analysis of the NIST 1950 plasma (Figure S4). In total the VJC system generated 3962 mass-retention time features from the NIST 1950 plasma compared to 3640 for the standard method (+ve ESI), an increase of ca. 9.0%. The number of lipid identifications was also higher using the VJC system rising from 734 by UHPLC to 820 with VJC (based on the Lipidblast database, +ve ESI). It is thus clear from these data that, despite the shallow nature of much of the gradient, the VJC system still provided higher chromatographic resolution than the conventional LC system.

VJC-UHPLC vs Conventional UHPLC: Rapid Gradient Analysis Using 30 and 50 mm Columns

Increasing throughput in LC-MS assays is often achieved by reducing column length and the concomitant geometric scaling of the gradient profile. Such an approach has been used to good effect as a means of significantly increasing throughput in disciplines such as bioanalysis and drug metabolite profiling/identification.[19,20] The same approach has also been demonstrated to be a successful strategy in omics,[21] especially when combined with a reduction in column internal diameter, allowing the mobile phase velocity to be increased without increasing the flow rate.[22] These rapid microbore metabolic profiling (RAMMP) methods,[23,24] including for lipidomic applications,[23] have been shown to deliver equivalent LC performance to the larger column geometry methods when the post column dispersion is correctly controlled. Therefore, to address the high throughput lipidomics challenge, the conventional and VJC systems were scaled to 50% and 33% of the original 10 min method by employing columns of 5 and 3 cm in length, respectively. The mobile phase flow rate was maintained at 0.5 mL/min and the gradient times reduced by 50 and 33% respectively, thereby keeping the number of column volumes which defined the gradient constant at 28, as used in the 10 min methodology. In theory the benefit of using the VJC approach is expected to be highest with a rapid analysis because the pre- and postcolumn dispersion values (σ) are a constant. Therefore, with short rapid gradients, where the peak volumes are small, the combined on-column and post column dispersion volumes represent a greater percentage of the peak volume than with a longer separation where the peak widths are greater. On the basis of the in-house modeling tool, we expected a 12 and 43% (shallow−steep sections of LC gradient, respectively) uplift in peak capacity for the 5 min analysis and a 16 and 82% (shallow−steep sections of LC gradient, respectively) increase for the 3 min analyses.

Initially the VJC and conventional UHPLC column/system methods were again compared using the "splash mix". This approach showed that, for a 5 min analysis on a 50 mm column, the VJC system continued to provide significantly narrower peaks than the conventional system (Figure S5). As an example, the PC lipid (m/z 753.6), detected using +ve ESI, had a peak width of 9 s on the standard UHPLC system which was reduced to 6 s on the VJC system. Similarly, the triglyceride and cholesterol ester lipids eluting at the end of the separation (m/z 834.7 and 369.3) showed a reduction in peak width from 12 s on the UHPLC system to 6 s with the VJC system (Figure S5). This provides a theoretical peak capacity of 50 for the VJC system when performing a 5 min analysis, which is almost exactly half of that obtained for the 10 min analysis and peak capacity of 25 for the UHPLC system. The peak tailing factors were reduced from 1.08 for the UHPLC

https://doi.org/10.1021/acs.jproteome.1c00836
J. Proteome Res. 2022, 21, 691−701

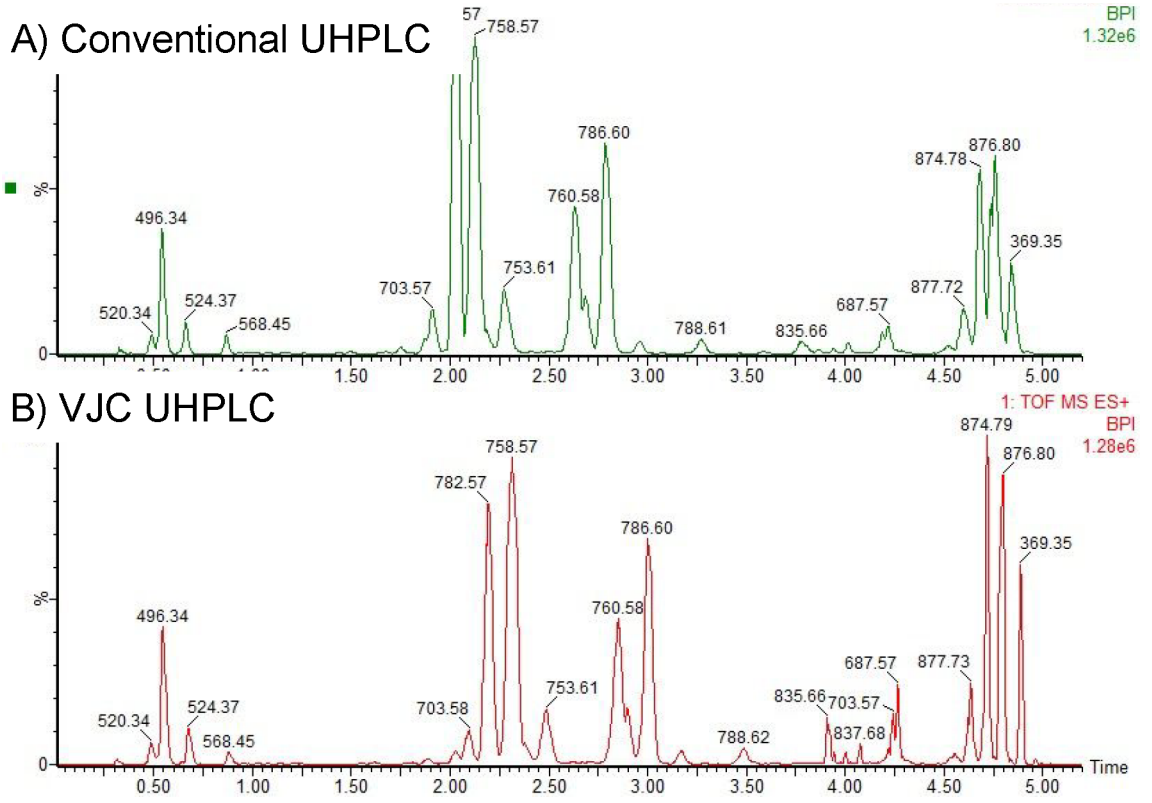

Figure 1. Comparison of mass chromatograms obtained from the UPLC-MS (+ve ESI) analysis of the NIST 1950 plasma (time scale in minutes). Upper trace (A): Data from the conventional method (ACQUITY UPLC CSH C18 1.8 μm 2.1 mm × 50 mm column). Lower trace (B): Data from the VJC method (ACQUITY UPLC CSH C18 1.8 μm 2.1 mm × 50 mm column).

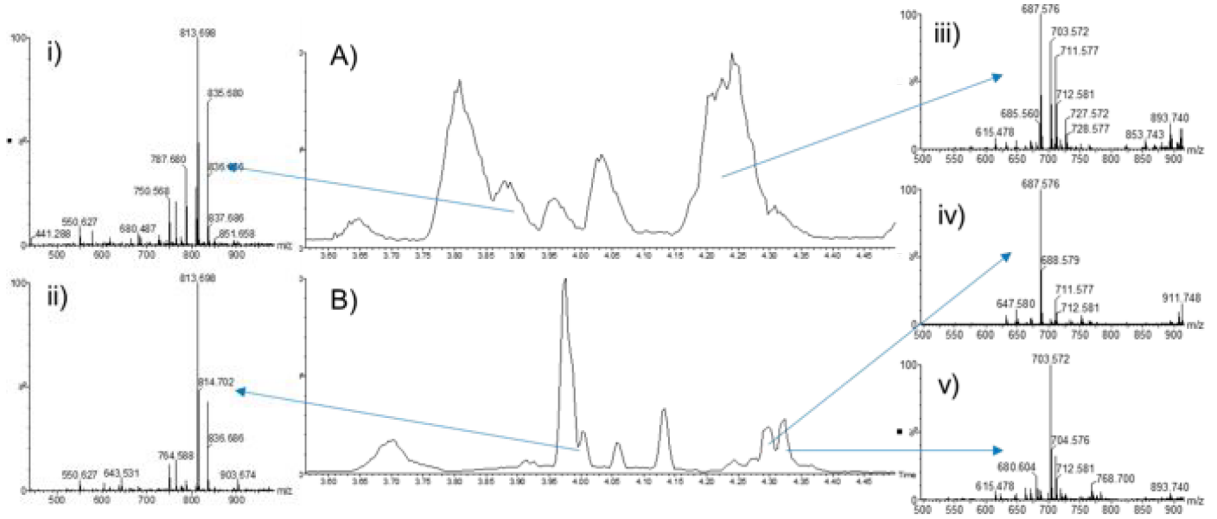

Figure 2. Comparison of mass chromatograms obtained from the UHPLC-MS (+ve ESI) analysis of the NIST 1950 plasma (time scale in minutes) using ACQUITY UPLC CSH C_{18} 1.7 μm 2.1 mm × 50 mm column and a 5 min gradient separation. Trace A: Data from the conventional method. Trace B: Data from the VJC method. Extracted ion MS spectra (i) and (ii) obtained from peak eluting at 3.9 min using UHPLC column, and 4.00 min on the VJC column, respectively. MS spectra (iii–v) obtained from peaks eluting at 4.25 on the UHPLC system and 4.30 and 4.33 on the VJC system, respectively.

system to 1.02 for the VJC system for the PC m/z 753.6 and from 1.67 to 1.10 (UHPLC vs VJC) for PC m/z 876.6, representing 2% and 34% reductions respectively. The analysis of the NIST 1950 plasma extract, also using +ve ESI and illustrated in Figure 1, revealed similar qualitative improvement in the separation of the lipid species: with the PC lipids (eluting between 1.7–2.5 min). A further example of the value of the VJC concept was the lipid m/z 703.6 (t_R 2.1 min), which was clearly resolved from other lipids in the VJC separation but coeluted with other analytes in the conventional UHPLC method. Similarly, more fine detail was revealed between 3.7–4.5 min using the VJC system, with the SM lipid m/z 837.68 appearing as a sharp peak, yet by conventional UHPLC was seen as a broad peak. It is also noteworthy that there was

https://doi.org/10.1021/acs.jproteome.1c00836
J. Proteome Res. 2022, 21, 691–701

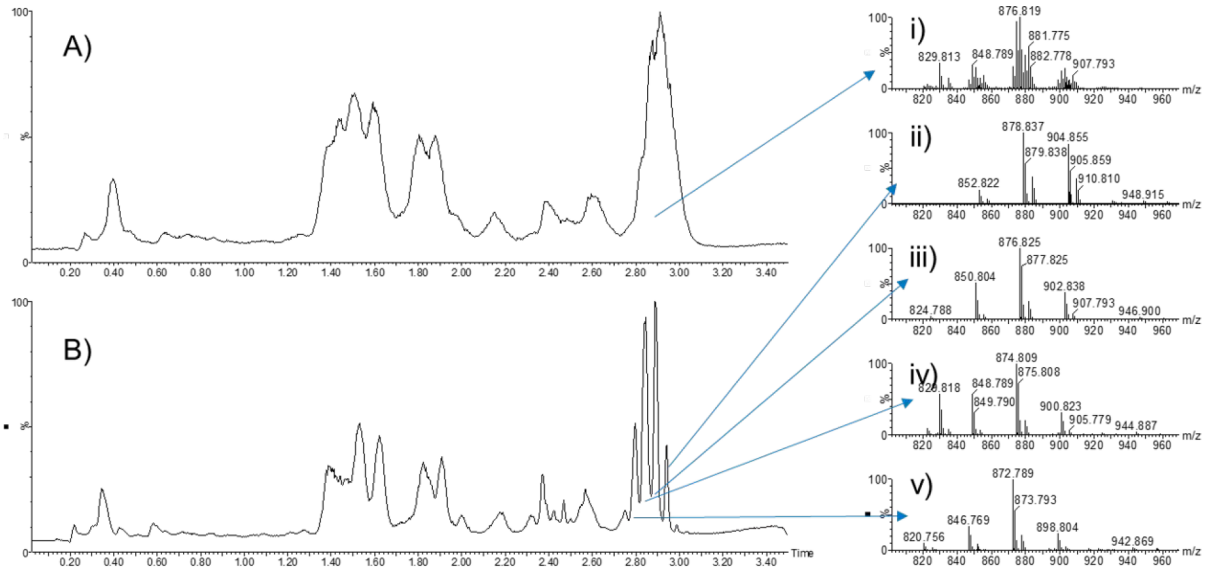

Figure 3. Comparison of mass chromatograms obtained from the UHPLC-MS (+ve ESI) analysis of the NIST 1950 plasma (time scale in minutes) using a 3 min gradient separation on ACQUITY CSH 2.1 mm × 30 mm C18 1.8 μm columns. Trace A: Data from the conventional method and B: Data from the VJC method. Extracted ion MS spectra (i) obtained from the peak eluting at 2.9 min using UHPLC column, MS spectra (ii–v) obtained from peaks eluting at between 2.75 and 3.0 min using the VJC system.

Table 2. Comparison of Chromatographic Performance between Conventional UHPLC and VJC 10, 5, and 3 min Analysis Using 100, 50, and 30 mm Columns, Respectively

component	UHPLC system (10 min)	VJC system (10 min)	UHPLC system (5 min)	VJC system (5 min)	UHPLC system (3 min)	VJC system (3 min)
peak width SM (sec)	12	9	9	6	7	3.6
peak width TG (sec)	8	4.5	6	2.4	5	2.4
peak capacity	65	100	30	50	22	45
number of features (NIST 1950) (+ve ESI)	3640	3962	2030	2683	1371	1649
number of identified lipids	734	820	460	541	311	371
peak intensity	3.5×10^5	7.1×10^5	5.96×10^5	7.45×10^5	4.56×10^5	5.7×10^5
peak tailing[a] (m/z 753.61)	1.37	1.05	1.08	1.02	1.16	1.00
peak tailing[a] (m/z 876.80)	1.33	1.08	1.67	1.16	1.50	1.20

[a]Peak tailing was determined on peaks at m/z 753.61 at t_R 4.58, 2.53, 1.48 min and m/z 876.8 at t_R 9.50, 4.71, 2.86 min for the 100, 50, and 30 mm columns, respectively.

significantly more fine detail for the CE lipid cluster eluting at ca. 4.3 min (m/z 687.58) on the VJC system compared to the conventional separation, Figure 2. The lipophilic triglycerides and cholesterol esters eluting towards the end of the gradient were also baseline resolved into 4 peaks using VJC, whereas they were an unresolved quartet of overlapping peaks by UHPLC.

Overall, 2030 features were found in the NIST 1950 extract by the UHPLC analysis with 2683 (a 32% increase) (+ve ESI) detected using VJC system. More importantly however, the improved resolution of the VJC system resulted in the number of lipid identifications (based on the Lipidblast database) increasing from the 460 obtained with the UHPLC system to 541 using VJC, representing a 19% increase for the latter.

The results for the 3 min analysis showed a similar pattern to that obtained for the 5 min analysis, with the VJC system providing superior resolution to standard UHPLC. As shown in Figure 3 the quartet of TG and cholesterol esters were still partially resolved with the VJC system but were merged into a cluster in the UHPLC separation. Again, there were greater than 50% reductions in peak widths when VJC was deployed compared to a standard system as detailed in Table 2. The resulting calculated peak capacity of the VJC system with a 3 min analysis was 45 compared to 20 for the UHPLC system. The peak tailing factors were reduced by 14% and 18% for the PC m/z 753.6 and TG m/z 876.8, respectively.

These chromatographic data are summarized below in Table 2; these were obtained from single determination using a QC sample which is representative of the composition of the test samples, with the same QC used for each column configuration. Plasma samples were analyzed in triplicate, enabling this QC to be consistent. The number of features observed using the 3 min separation on the 30 mm column increased from 1371 for the UHPLC system to 1649 (+ve ESI) with the VJC system (a 20.3% increase), while the number of lipid identifications increased from 311 with the UPLC system to 371 with the VJC system (Lipidblast identifications).

Effects of VJC on MS Spectral Quality

As described above the increased chromatographic peak capacity produced by the VJC system facilitated improved resolution between lipids which were unresolved on the UHPLC system. This increased peak resolution produced a significant improvement in the MS and MS/MS spectra

https://doi.org/10.1021/acs.jproteome.1c00836
J. Proteome Res. 2022, 21, 691−701

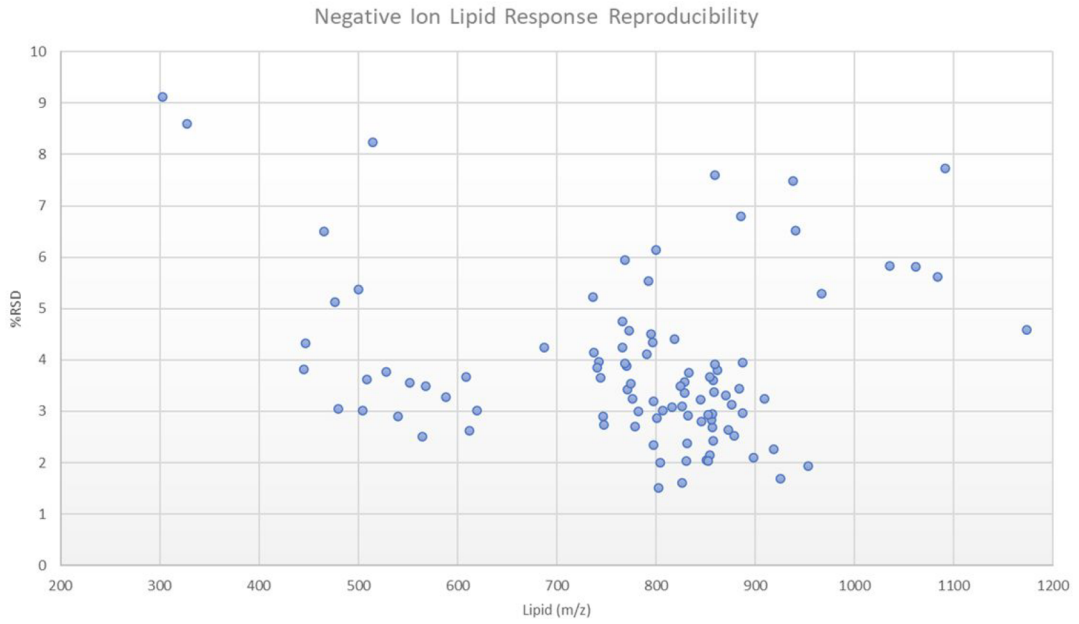

Figure 4. Comparison of RSD of peak response for 100 lipids eluting between 0.35 and 9 min on VJC system in −ve ESI.

derived from the chromatographic peaks. For example, the 10 min separation of the positive ion LC-MS analysis of the NIST plasma provided much clearer MS spectra for the peak eluting at t_R 3.7 min on the VJC system compared to those obtained by UHPLC-MS (Figure S6). As shown here the VJC separation gave rise to a simple spectrum for the lipid m/z 829.548 (BPI m/z 806.566) compared to the conventional UHPLC system where the spectra from two lipids were merged, and with the data also containing ions from the m/z 725.554 lipid. A similar result was obtained for the lipids eluting at t_R 4.1 min on the UHPLC system and t_R 4.4 min on the VJC system. Thus, from the spectra shown in the inset to Figure S7 it is obvious that the UHPLC system provided a combined signal from two coeluting lipids (m/z 736.656 and m/z 782.584), whereas the VJC system clearly resolved them, giving rise to much simpler, and easier to interpret spectra. This improved spectral quality obtained from the VJC system was most significant toward the end of the chromatographic analysis where the solvent gradient was at its steepest. This effect is illustrated by the results for two TG lipids, eluting at t_R 9.4 min with m/z 829.818 and m/z 874.809. These two lipids were unresolved by UHPLC, giving rise to MS data which was an amalgam of fragments derived from both. In contrast these two lipids were well resolved on the VJC system, providing two discrete, clean spectra (Figure S8). The sharper peaks produced by the VJC system for these TG also resulted in an almost 2-fold increase in MS peak response compared to that obtained using UHPLC (Figure S9).

The improvement in MS spectral quality delivered by VJC compared to the conventional UHPLC was also observed with the 5 min separation. The data displayed in Figure 2 illustrate the improvement in spectral clarity obtained for the VJC system for the lipid species eluting between 3.7 and 4.4 min. It can be seen from these data that the peak eluting at 3.9 min on the UHPLC system was resolved into two peaks on the VJC system. A comparison of the derived MS spectra showed that the UHPLC system (A) produced an MS spectrum which contained signals from several lipids (i), whereas the VJC system (B) produced a much clearer and easier to interpret MS spectrum from a single lipid (ii). A similar observation can be made for the peak eluting at 4.25 min, which appeared to be a single peak in the UHPLC chromatogram but was resolved into two discrete peaks using the VJC system. The MS spectrum produced by the UHPLC system (iii) showed a combination of the two lipids m/z 687.576 and m/z 703.572, in contrast the two peaks produced by the VJC system contain the spectra for the individual lipids, with the m/z 687.576 lipid (iv) eluting first followed by the m/z 703.572 lipid (v).

This improvement in VJC spectral data quality was also observed for the high collision energy data, as illustrated by the lipid peak eluting at 4.0 min in the bovine liver extract, which was also examined in this study, using the 5 min analysis (mass chromatogram shown in Figure S10). It is clear from the data in Figure S11 that although the low collision energy data were similar (Figures S11A,C) for the VJC and UHPLC systems, the high energy MS data derived from the VJC system (Figure S11B) was much cleaner, and therefore easier to interpret, than the spectra obtained for the high energy MS data generated by UHPLC under the same conditions (Figure S 11D). This effect was evident to an even greater extent with the 3 min VJC vs UHPLC data from the +ve ESI analysis of the NIST 1950 plasma extract where the TGs were eluted as one unresolved peak in the UHPLC, giving rise to a composite MS spectrum containing signals from all of the TGs (i) (Figure 3). In contrast, using the VJC under the same conditions, the TGs were resolved into 4 peaks (ii−v), with an elution order of m/z 872.789, m/z 874.809, m/z 876.825, and m/z 878.837, respectively, with each providing a clear, readily interpreted spectrum.

Application to Mouse Plasma Following Administration of Gefitinib

Having evaluated the VJC system on the NIST 1950 plasma and the Avanti liver extract and shown it to generate superior data to conventional UHPLC-MS, it was then applied to mouse plasma samples obtained from mice dosed with gefitinib.[15] Mouse plasma samples obtained from both IV and PO dosed animals were analyzed in triplicate by UHPLC

https://doi.org/10.1021/acs.jproteome.1c00836
J. Proteome Res. 2022, 21, 691−701

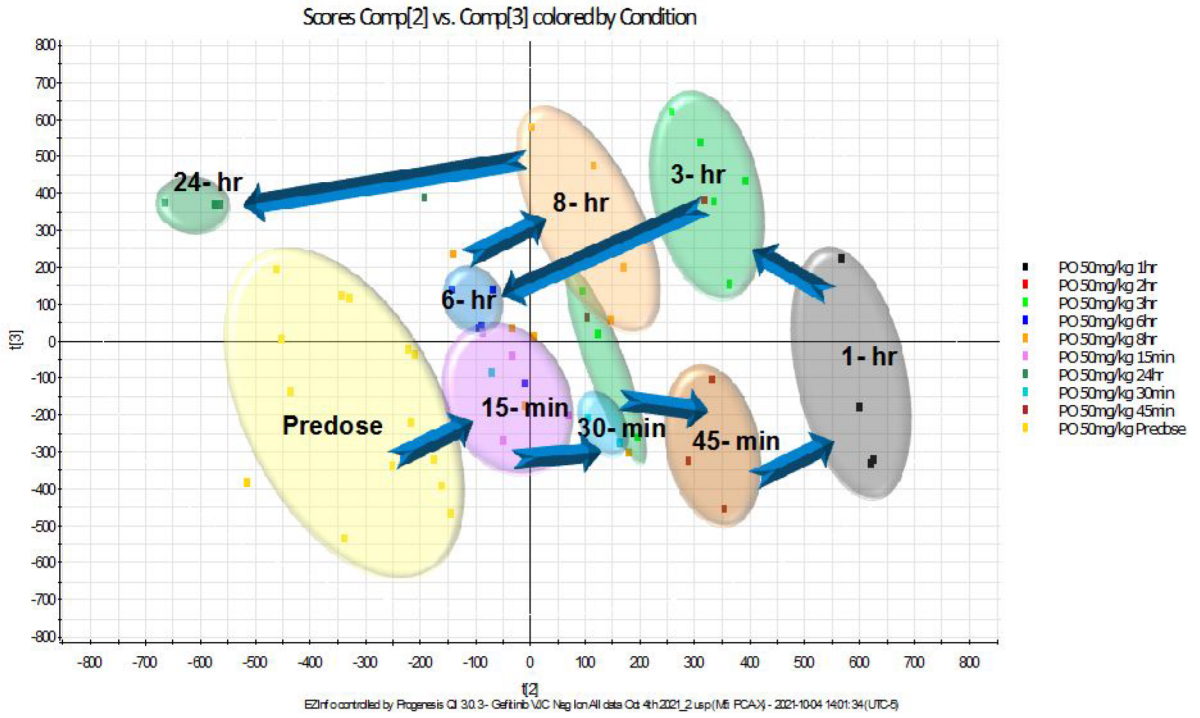

Figure 5. Principal component analysis (PCA) plot of the third (PC3) versus the second (PC2) principal components of the gefitinib mouse plasma extract following PO dosing at 50 mg/kg VJC LC-MS analysis (−ve ESI). PC2 accounted for 16% of the variance in the data with PC3 accounting for 11% of the variance in the data.

and VJC in both +ve and −ve ESI providing an analytical run, for each mode of ionization, comprised of ca. 300 individual LC-MS analyses including pooled QCs. The data presented here were derived from analyses conducted using a 5 min analysis with a 50 mm long column. Representative mass chromatograms for the pool QC obtained with the conventional UPLC and VJC systems in both +ve and −ve ESI are shown in Figures S12 and S13, respectively. As expected, the data obtained showed a clear improvement in the quality of the LC-MS separation obtained using the VJC system. An examination of the QC data showed that there was no degradation in the quality of the separation between the first and last QC sample. To illustrate this, the %RSD for the peak response of the lipids was evaluated for the 4000 detected features in the pooled QC samples where the RSD (n = 14) ranged from 1.8 to 9.7% for −ve ESI, and 1.5 to 12.6% in +ve ESI. The data displayed in Figure 4 show the variation of the RSD (n = 14) for 100 lipids, with representatives from each class of lipids, across a range of molecular masses monitored in −ve ESI. In these data the RSD ranged from 1.5 to 10%.

When the data for the plasma samples obtained following IV dosing of gefitinib (10 mg/kg) for the period from predose to 24 h postdose were analyzed statistically by PCA, the score plots obtained from the data obtained for both UHPLC and VJC platforms showed discrimination between the time points as illustrated in (Figures S14, S15). The data suggested that the VJC LC-MS analysis provided tighter clustering of the statistical data points. Under the chromatographic conditions used here, the drug and its metabolites were eluted as a combined peak near the solvent front and were easily excluded from any statistical analysis. Therefore, the differences highlighted by the PCA seen here resulted from changes in lipid composition as a consequence of the administration of the drug. The individual time points and QC samples were clearly separated using the data from the UHPLC-MS analysis, with, e.g., PC1 and PC2 (for +ve ESI) accounting for 23% and 17% of the observed variance in these data, respectively. As can be seen from the PCA score plot for the VJC separation, the samples showed a clear, time-related response to gefitinib administration. Thus, the trajectory moved rapidly away from the predose samples, with the 2 and 3 h samples clustering closely together and the 24 h samples returning to a position nearer to that occupied by the predose samples.

A not dissimilar result was obtained for the samples from mice following PO administration of 50 mg/kg of gefitinib. The PCA scores plot from the VJC LC-MS analysis, shown in Figure 5, indicates a clear lipidomic response, rapidly moving away from the predose samples toward the 1 h samples, with a slow return to almost the original starting position by 24 h postdose. As can be seen the PCA data obtained for the IV and PO routes revealed a very complex pattern in the variance (Figures 5 and S14, S15). This variance may be attributed to the metabolic effects of drug administration combined with other factors such as, e.g., diurnal variation, effects of feeding, animal handling and environmental effects contributing to, e.g., cage effects. It can therefore be hypothesized that there are multiple dimensions of separation in metabolic hyperspace which are difficult to easily visualize in a simple 2- or even the 3-dimensional PCA plot shown in Figure S16 for the 50 mg/kg dosed mice. Previous studies, Molloy et al.,[15] McKillop et al.,[25] Zheng et al.[26] have shown that the T_{max} for gefitinib and the drug related metabolites, O-desmethyl (M523595), morpholino carbonyl (M605211), and desfluoro-phenol (M387783) occur between 0.75 and 1-h postdose following PO administration, with a significant concentration remaining at the 3 h time point. This information combined with pharmacometabodynamic analysis[27] of urine from the same study identified that endogenous biochemical markers of

https://doi.org/10.1021/acs.jproteome.1c00836
J. Proteome Res. 2022, 21, 691−701

dysregulation in the urine also showing a maximum in the 3 to 4 h postdose time region. Thus, to simplify the analysis and data visualization, the +ve ESI data for the 2- and 3-h postdose PO and vehicle dosed animal samples were subject to PCA analysis. The resulting 3D plot of PC 1 vs PC2 vs PC3 is given in Figure 6. On the basis of the data obtained, a clear separation between the predose and 3 h PO samples, which was not observed for the vehicle dosed animals, can be seen suggesting that the dosing of gefitinib is associated with "pharmacological" effects on the circulating lipids. These two time points were subject to Orthogonal Projections to Latent Structures Discriminant Analysis (OPLS-DA) and the signals which contributed most significantly to the observed variance were derived from the S-Plot. The lipids species which showed either up or down regulation in the 3 h PO dosed group in the MVA analysis are summarized in Table 3. These lipids were identified using database searching of accurate mass of their precursor ion, fragment ion match and isotopic pattern, an example spectrum of lipid PE 18:0 22:6 is given in Figure S17.

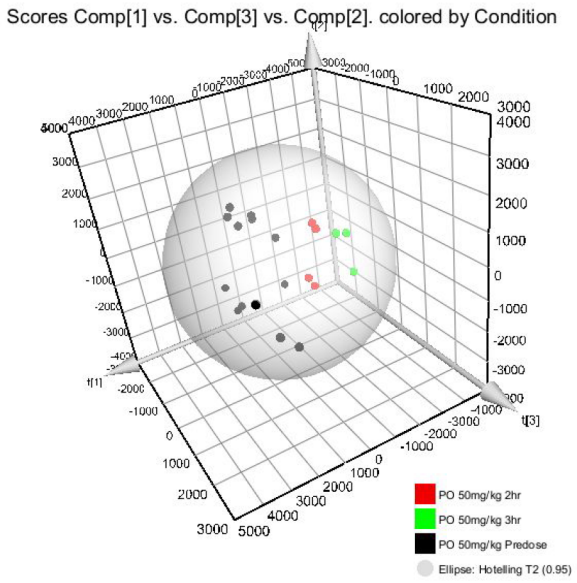

Figure 6. Principal component analysis (PCA) plots (PC1 vs PC2 vs PC3) of principal components of the gefitinib mouse plasma extract following PO dosing at 50 mg/kg VJC LC-MS analysis (+ve ESI). PC1, PC2, and PC3 accounted for 23%, 17%, and 10% of the variance in the data, respectively.

The major classes of lipids which showed changes in their regulation were the LPC's, PC's, PE's, and PI's (Table 3). These changes are intriguing and may give a mechanistic insight into the mode of action of gefitinib. This will be discussed in more detail in subsequent publications, in conjunction with the metabolic phenotyping of the livers of these animals.

The original studies applying UHPLC-MS to metabolic phenotyping showed a clear benefit in terms of increased chromatographic efficiency, providing both sharper and more intense peaks than conventional HPLC-MS, and significantly greater numbers of them.[28] This combination of beneficial features initially resulted in many investigators essentially substituting their existing HPLC separations with similar ones based on UHPLC. However, even then, the utility of rapid analyses based on UHPLC with fast gradients, so as to increase sample throughput with an equivalent peak count to the conventional methods, was also clear.[29] The limiting factor in early applications of the rapid gradient profiling approach was, however, that extra-column band broadening was not fully addressed, reducing the effective peak capacity obtained. Subsequently such issues were resolved, at least partially, by the development of the so-called "RAMMP" methods,[22−24] where the connections from the column to the ion source of the mass spectrometer were optimized. However, while providing a significant improvement in peak shape via the mitigation of extra-column band broadening RAMMP did not compensate for the on-column effects of frictional heating. As we have recently shown for more polar metabolites,[14] and as demonstrated here for lipids, the use of the VJC concept to simultaneously reduce both on-column and postcolumn band broadening effects brings significant benefits to rapid gradient-based methods and can provide incremental improvements for longer gradient analyses. The use of VJCs may therefore represent an important step in maximizing the benefits of UHPLC in complex mixture analysis for metabonomic/metabolomics, lipidomics, and proteomics.

CONCLUSIONS

Vacuum jacketed columns (VJC) located at the source of the mass spectrometer show great potential for increasing both information recovery and throughput in LC-MS-based lipidomic analysis of plasma extracts. The VJC system demonstrated an 8−20% increase in resolving power for the 10, 5, and 3 min methods compared to the similar geometry conventional system, significantly improving the resolution of

Table 3. Lipids Identified as Up- or Down-Regulated in the Plasma of Mice Administered 50 mg/kg PO with the EGFR Inhibitor Gefitinib

description	up/down-regulated	fold change	ANOVA *p*-value	*m/z*	retention time (min)	score	fragmentation score	mass error (ppm)	isotope similarity
LPC(16:0)	↓	1.06	0.147	540.3305	0.53	57.2	88	−0.43	98.73
LPC(18:2)	↑	1.09	0.070	564.3303	0.47	47.2	56.8	−0.69	80.13
LPC(20:4)	↑	1.22	0.185	588.3299	0.46	41.4	25.8	−1.52	82.88
LPC(22:6)	↑	1.30	0.019	612.3302	0.44	52.2	69.7	−0.92	92.49
LPE(18:2)	↓	1.16	0.035	476.2766	0.49	51.4	77.6	−3.52	83.26
LPE(22:0)	↓	1.36	0.001	582.3759	0.74	50.7	59.3	−3.31	98.38
PC(16:0_20:4)	↑	1.23	0.017	826.5604	2.14	52.1	66.8	0.02	93.50
PC(16:0_22:6)	↑	1.16	0.001	850.5609	1.97	57.9	93	0.62	97.22
PC(18:0_18:2)	↓	1.04	0.227	830.5918	2.95	58.4	93.7	0.17	98.36
PC(18:0_18:2)	↓	1.14	0.001	784.5842	3.27	41.9	16.9	−2.46	95.45

https://doi.org/10.1021/acs.jproteome.1c00836
J. Proteome Res. 2022, 21, 691−701

the SM and TG lipids. A 5 min reversed-phase VJC LC-MS method yielded peak widths as low as 2.4 s at the base and a peak capacity of 50 compared to 30 for the non-VJC, system. The enhanced resolution obtained with the VJC also resulted in a 32% increase in feature detection and a 22% increase in identified lipids. The increase in resolving power of the VJC system compared to the conventional UHPLC system became more significant as the column length and analysis time were reduced, with the 3 min, 30 mm column, VJC method showing enhanced resolution of the TG's, whereas they eluted unresolved from the conventional system. The 3 and 5 min VJC-based methods also provided excellent metabolic phenotyping data with the former providing a 20% increase in the number of features detected compared to the similar geometry conventional system. The narrower peaks and increased resolution of the VJC systems (10, 5, and 3 min) resulted in cleaner, easier to interpret mass spectra throughout the chromatogram. The narrower VJC peaks also resulted in more intense peaks which is especially important for bioactive lipids, such as PA's and PS's, that are only present at low concentrations. The application of the VJC technology to the analysis of mouse plasma from the PO/IV administration of gefitinib provided evidence of changes in circulating lipid composition as a result of the pharmacological effects of the drug.

■ ASSOCIATED CONTENT

Supporting Information

The Supporting Information is available free of charge at https://pubs.acs.org/doi/10.1021/acs.jproteome.1c00836.

Figure S1: Mass chromatograms for the Avanti Polar Splash Mix; Figure S2: Comparison of mass chromatograms for NIST 1950 plasma for conventional vs VJC methods; Figure S3: Comparison of mass chromatograms for NIST 1950 plasma between 5.1 and 9 min for conventional vs VJC methods; Figure S4: Comparison of mass chromatograms obtained for TGs in NIST 1950 plasma by conventional and VJC methods; Figure S5: Comparison of mass chromatograms for the Avanti Polar Splash Mix for conventional and VJC methods; Figure S6: Comparison of extracted ion chromatograms (m/z 829.546) for a peak eluting at 3.7 min using conventional and VJC methods; Figure S7 and S8: Comparison of extracted ion chromatograms for peaks eluting at 4.1 min and 9.4 min (m/z 736.656, m/z 736.656, respectively) on conventional and VJC systems; Figure S9: Comparison of peak responses obtained for a TG (m/z = 850.804) via conventional and VJC methods; Figure S10: Comparison of the bovine liver extract mass chromatograms obtained with conventional and VJC methodologies; Figure S11: High and low collision energy spectra (+ve ESI) for the bovine liver obtained via conventional UHPLC and VJC methods; Figure S12 and S13: Comparisons of mass chromatograms (+ve ESI and −ve ESI) obtained for mouse QC plasma for conventional and VJC methods; Figure S14 and S15: PCA (ESI+) of PC1 versus PC2 of gefitinib mouse plasma and PC1 versus PC3 for gefitinib mouse plasma (IV, 10 mg/kg) following conventional analysis (ESI+); Figure S16: PCA plot of gefitinib mouse plasma (PO, 50 mg/kg) following VJC/LC-MS analysis (ESI−); Figure S17: Lipid Database search of PE16:0 22:6 (m/z 790.5389) after VJC analysis (PDF)

■ AUTHOR INFORMATION

Corresponding Author

Robert S. Plumb − *Scientific Operations, Waters Corporation, IMMERSE, Cambridge, Massachusetts 02142, United States;* orcid.org/0000-0002-1380-9285; Email: rob_plumb@waters.com

Authors

Giorgis Isaac − *Scientific Operations, Waters Corporation, IMMERSE, Cambridge, Massachusetts 02142, United States*

Paul D. Rainville − *Scientific Operations, Waters Corporation, IMMERSE, Cambridge, Massachusetts 02142, United States*

Jason Hill − *Global Research, Waters Corporation, IMMERSE, Cambridge, Massachusetts 02142, United States*

Lee A. Gethings − *Scientific Operations, Waters Corporation, Wilmslow SK9 4AX, U.K.*

Kelly A. Johnson − *Global Research, Waters Corporation, IMMERSE, Cambridge, Massachusetts 02142, United States*

Joshua Lauterbach − *Department of Chemistry, University of Massachusetts Amherst, Amherst, Massachusetts 01003, United States*

Ian D. Wilson − *Computational & Systems Medicine, Department of Metabolism, Digestion and Reproduction, Imperial College, London SW7 2AZ, U.K.;* orcid.org/0000-0002-8558-7394

Complete contact information is available at: https://pubs.acs.org/10.1021/acs.jproteome.1c00836

Notes

The authors declare no competing financial interest.

■ REFERENCES

(1) Stace, C. L.; Ktistakis, N. T. Phosphatidic Acid- and Phosphatidylserine-binding Proteins. *Biochim. Biophys. Acta, Mol. Cell Biol. Lipids* **2006**, *1761*, 913−926.

(2) Han, X. Lipidomics for Studying Metabolism. *Nat. Rev. Endocrinol.* **2016**, *12*, 668−679.

(3) Meikle, P. J.; Wong, G.; Barlow, C. K.; Kingwell, B. A. Lipidomics: Potential Role in Risk Prediction and Therapeutic Monitoring for Diabetes and Cardiovascular Disease. *Pharmacol. Ther.* **2014**, *143*, 12−23.

(4) Eghlimi, R.; Shi, X.; Hrovat, J.; Xi, B.; Gu, H. Triple Negative Breast Cancer Detection Using LC-MS/MS Lipidomic Profiling. *J. Proteome Res.* **2020**, *19*, 2367−2378.

(5) Xuan, Q.; Hu, C.; Yu, D.; Wang, L.; Zhou, Y.; Zhao, X.; Li, Q.; Hou, X.; Xu, G. Development of a High Coverage Pseudotargeted Lipidomics Method Based on Ultra-High Performance Liquid Chromatography-Mass Spectrometry. *Anal. Chem.* **2018**, *90*, 7608−7616.

(6) Chew, W. S.; Torta, F.; Ji, S.; Choi, H.; Begum, H.; Sim, X.; Khoo, C. M.; Khoo, E.; Ong, W. Y.; Van Dam, R. M.; Wenk, M. R.; Tai, E. S.; Herr, D. R. Large-scale Lipidomics Identifies Associations Between Plasma Sphingolipids and T2DM Incidence. *JCI Insight.* **2019**, *5*, e126925.

(7) Xu, T.; Hu, C.; Xuan, Q.; Xu, G. Recent Advances in Analytical Strategies for Mass Spectrometry-based Lipidomics. *Anal. Chim. Acta* **2020**, *1137*, 156−169.

(8) Cífková, E.; Hájek, R.; Lísa, M.; Holcapek, M. Hydrophilic Interaction Liquid Chromatography-mass Spectrometry of Lysophosphatidic acids, Lysophosphatidylserines and Other Lipid classes. *J. Chromatogr. A* **2016**, *1439*, 65−73.

(9) Damen, C. W.; Isaac, G.; Langridge, J.; Hankemeier, T.; Vreeken, R. J. Enhanced Lipid Isomer Separation in Human Plasma Using Reversed-phase UPLC with High-Resolution Ion-mobility MS Detection. *J. Lipid Res.* **2014**, *55*, 1772−1783.
(10) Rainville, P. D.; Murphy, J. P.; Tomany, M.; Wilson, I. D.; Smith, N. W.; Evans, C.; Kheler, J.; Bowen, C.; Plumb, R. S.; Nicholson, J. K. An Integrated Ceramic, Micro-fluidic Device for the LC-MS/MS Analysis of Pharmaceuticals in Plasma. *Analyst* **2015**, *140*, 5546−5556.
(11) Gritti, F.; Gilar, M.; Jarrel, J. A. Achieving Quasi-adiabatic Thermal Environment to Maximize Resolution Power in Very High-pressure Liquid Chromatography: Theory, Models, and Experiments. *J. Chromatogr. A* **2016**, *1444*, 86−98.
(12) Gritti, F.; Gilar, M.; Jarrell, J. A. Quasi-adiabatic Vacuum-based Column Housing for Very High-pressure Liquid Chromatography. *J. Chrom. A* **2016**, *1456*, 226−234.
(13) Gritti, F. Designing Vacuum-Jacketed User-Friendly Columns for Maximum Resolution Under Extreme UHPLC and SFC Conditions. *LCGC* **2018**, *2018* (36), 18−23.
(14) Plumb, R. S.; McDonald, T.; Rainville, P. D.; Hill, J.; Gethings, L. A.; Johnson, K. A.; Wilson, I. D. High-Throughput UHPLC-MS/MS-Based Metabolic Profiling Using a Vacuum Jacketed Column. *Anal. Chem.* **2021**, *93*, 10644−10652.
(15) Molloy, B. J.; King, A.; Mullin, L. G.; Gethings, L. A.; Riley, R.; Plumb, R. S.; Wilson, I. D. Rapid Determination of the Pharmacokinetics and Metabolic Fate of Gefitinib in the Mouse Using a Combination of UPLC-MS/MS, UPLC/QToF/MS, and Ion Mobility (IM)-enabled UPLC/QToF/MS. *Xenobiotica* **2021**, *51*, 434−446.
(16) Sangster, T.; Major, H.; Plumb, R.; Wilson, A. J.; Wilson, I. D. A Pragmatic and Readily Implemented Quality Control Strategy for HPLC-MS and GC-MS-Based Metabonomic Analysis. *Analyst* **2006**, *131*, 1075−1078.
(17) Isaac, G. Electrospray Ionization Tandem Mass Spectrometry (ESI-MS/MS)-Based Shotgun Lipidomics. *Methods Mol. Biol.* **2011**, *708*, 259−275.
(18) Vorkas, P. A.; Isaac, G. M.; Anwar, A.; Davies, A. H.; Want, E. J.; Nicholson, J. K.; Holmes, E. Untargeted UPLC-MS Profiling Pipeline to Expand Tissue Metabolome Coverage: Application to Cardiovascular Disease. *Anal. Chem.* **2015**, *87*, 4184−4193.
(19) Meng, M.; Wang, L.; Voelker, T.; Reuschel; Van Horne, S. K.; Bennett, P. A Systematic Approach for Developing a Robust LC-MS/MS Method for Bioanalysis. *Bioanalysis* **2013**, *5*, 91−115.
(20) Ackermann, B. L.; Berna, M. J.; Murphy, A. T. Recent Advances in Use of LC-MS/MS for Quantitative High-throughput Bioanalytical Support of Drug Discovery. *Curr. Top Med. Chem.* **2002**, *2*, 53−66.
(21) Gika, H.; Virgiliou, C.; Theodoridis, G.; Plumb, R. S.; Wilson, I. D. Untargeted LC-MS-based Metabolic Phenotyping (Metabonomics/Metabolomics): The State of the Art. *J. Chromatogr. B: Anal. Technol. Biomed. Life Sci.* **2019**, *1117*, 136−147.
(22) Gray, N.; Adesina-Georgiadis, K.; Chekmeneva, E.; Plumb, R. S.; Wilson, I. D.; Nicholson, J. K. Development of a Rapid Microbore Metabolic Profiling Ultraperformance Liquid Chromatography-Mass Spectrometry Approach for High-Throughput Phenotyping Studies. *Anal. Chem.* **2016**, *88*, 5742−5751.
(23) King, A. M.; Trengove, R. D.; Mullin, L. G.; Rainville, P. D.; Isaac, G.; Plumb, R. S.; Gethings, L. A.; Wilson, I. D. Rapid Profiling Method for the Analysis of Lipids in Human Plasma Using Ion Mobility Enabled-reversed Phase-ultra High Performance Liquid Chromatography/Mass Spectrometry. *J. Chromatogr. A* **2020**, *1611*, 460597.
(24) King, A. M.; Mullin, L. G.; Wilson, I. D.; Coen, M.; Rainville, P. D.; Plumb, R. S.; Gethings, L. A.; Maker, G.; Trengove, R. Development of a Rapid Profiling Method for the Analysis of Polar Analytes in Urine using HILIC-MS and Ion Mobility Enabled HILIC-MS. *Metabolomics* **2019**, *15*, 17.
(25) McKillop, D.; Hutchison, M.; Partridge, E. A.; Bushby, N.; Cooper, C. M.; Clarkson-Jones, J. A.; Herron, W.; Swaisland, H. C. Metabolic Disposition of Gefitinib, an Epidermal Growth Factor Receptor Tyrosine Kinase Inhibitor, in Rat, Dog and Man. *Xenobiotica* **2004**, *34*, 917−934.
(26) Zheng, N.; Zhao, C. X.; He, R. S.; Jiang, T. S.; Han, Y.; Xu, G. B.; Li, P. P. Simultaneous Determination of Gefitinib and its Major Metabolites in Mouse Plasma by HPLC-MS/MS and its Application to a Pharmacokinetics study. *J. Chromatogr. B: Anal. Technol. Biomed. Life Sci.* **2016**, *1011*, 215−222.
(27) Molloy, B.; Mullin, L.; King, A.; Gethings, L. A.; Plumb, R. S.; Wilson, I. D. The Pharmacometabodynamics of Gefitinib after Intravenous Administration to Mice: A Preliminary UPLC-IM-MS Study. *Metabolites* **2021**, *11*, 379.
(28) Wilson, I. D.; Nicholson, J. K.; Castro-Perez, J.; Granger, J. H.; Johnson, K. A.; Smith, B. W.; Plumb, R. S. High Resolution "Ultra Performance" Liquid Chromatography Coupled to oa-TOF Mass Spectrometry as a Tool for Differential Metabolic Pathway Profiling in Functional Genomic Studies. *J. Proteome Res.* **2005**, *4*, 591−598.
(29) Plumb, R. S.; Granger, J. H.; Stumpf, C. L.; Johnson, K. J.; Smith, B. W.; Gaulitz, S.; Wilson, I. D.; Castro-Perez, J. A Rapid Screening Approach to Metabonomics Using UPLC and oa-TOF Mass Spectrometry: Application to Age, Gender and Diurnal Variation in Normal/Zucker Obese Rats and Black, White and Nude mice. *Analyst* **2005**, *130*, 844−849.

https://doi.org/10.1021/acs.jproteome.1c00836
J. Proteome Res. 2022, 21, 691−701